Ecological Modelling, 65 (1993) 51–70
Elsevier Science Publishers B.V., Amsterdam

A simulation model for the transient effects of climate change on forest landscapes

I. Colin Prentice [a,1], Martin T. Sykes [a,1] and Wolfgang Cramer [b]

[a] *Department of Ecological Botany, Uppsala University, Box 559, S-751 22 Uppsala, Sweden,*
[b] *Department of Geography, University of Trondheim (AVH), N-7055 Dragvoll, Norway*

(Received 12 March 1991; accepted 13 March 1992)

ABSTRACT

Prentice, I.C., Sykes, M.T. and Cramer, W., 1993. A simulation model for the transient effects of climate change on forest landscapes. *Ecol. Modelling*, 65: 51–70.

Forests are likely to show complex transient responses to rapid changes in climate. The model described here simulates the dynamics of forest landscapes in a changing environment with simple phenomenological equations for tree growth processes and local environmental feedbacks. Tree establishment and growth rates are modified by species-specific functions describing the effects of winter and summer temperature limitations, accumulated annual foliage net assimilation and sapwood respiration as functions of temperature, CO_2 fertilization, and growing-season drought. These functions provide external conditions for the simulation of patch-scale forest dynamics by a forest succession model, FORSKA, in which all of the trees on each 0.1 ha patch interact by competition for light and nutrients. The landscape is simulated as an array of such patches. The probability of disturbance on a patch is a power function of time since disturbance. Forest structure, composition and biomass simulated for the landscape average in boreal and temperate deciduous forests approach reasonable equilibrium values in 200–400 years. A climatic warning scenario is applied to central Sweden, where temperature and precipitation increases are shown to interact with each other and with soil water capacity in determining the transient and equilibrium responses of the forest landscape to climate change.

INTRODUCTION

Climate changes during the past 10^4 years have affected the distribution of different forest types worldwide (Huntley and Webb, 1988; Prentice,

Correspondence to: I.C. Prentice, Department of Plant Ecology, Lund University, Östra Vallgatan 14, S-223 61 Lund, Sweden.
[1] Present address: Department of Plant Ecology, Lund University, Östra Vallgatan 14, S-223 61 Lund, Sweden.

1991) and changes of a comparable magnitude are likely to occur—but at a faster rate—during the next 100–200 years as a consequence of the greenhouse effect (Bolin et al., 1986; Houghton et al., 1990). Such rapid climate changes may exceed the rate at which the species composition, production and biomass of forest landscapes can remain in dynamic equilibrium with the environment, and complex transient responses may occur (Prentice et al., 1991a). A model to simulate these transient responses must incorporate the effects of a changing environment on different tree species (allogenic processes), the internal dynamics of the forest (autogenic processes), and the interactions between these two types of process. It should be able to simulate these basic dynamics correctly for a wide range of forest types, including the directional succession shown by most boreal forests as well as the quasi-cyclical "gap-phase replacement" dynamics shown by many temperate and tropical forests (Bonan and Shugart, 1989; Prentice and Leemans, 1990).

Natural disturbance is also an essential component of forest dynamics. Forested landscapes include patches that have been disturbed by natural causes (such as fire and windthrow), or by timber harvesting, at different times in the past. The process that gives rise to the spatial distribution of time-since-disturbance across patches is the *disturbance regime* (White, 1979; Pickett and White, 1985). The disturbance regime must be incorporated into models designed to predict the behaviour of large areas of forest, rather than individual forest stands. Although small patches of forest show intrinsically non-equilibrium behaviour, the existence of a disturbance regime allows the forest to approach equilibrium on a larger scale provided the climate remains constant (Pickett and Thompson, 1978; Pickett, 1980; Shugart, 1984; Prentice, 1991)—or more precisely, so long as the climate changes slowly relative to the rate at which the landscape approaches equilibrium (Webb, 1986; Prentice, 1991; Prentice et al., 1991b). Simulated equilibrium states of the landscape in a stationary climate provide convenient starting points for the simulation of transient responses to climate change.

We describe a model for forest landscape dynamics based on these principles. At its core is a "gap model" (Shugart, 1984) that simulates the autogenic dynamics of forest vegetation, including succession and gap-phase replacement, based on simple phenomenological relationships describing tree form and growth, the collective effect of trees on their immediate (patch) environment, the responses of tree growth to the patch environment, and changes in establishment and mortality rates associated with changes in growth. The particular gap model used is a version of FORSKA (Prentice and Leemans, 1990; Leemans, 1991a), a general-purpose gap model that has been shown to produce appropriate dynamics in boreal,

temperate and tropical forests (Prentice and Leemans, 1990; Leemans, 1991b; Desanker and Prentice, 1991). This core model takes care of the interactions between the tree canopy and the labile aspects of the local patch environment (light and nutrients). The core model is forced by a series of environmental modules which translate monthly climate and other environmental data into scalars influencing the establishment and growth rates of tree species. Species-specific functions convert the current values of these scalars into multipliers in the process equations of FORSKA. The forest landscape is simulated as an array of replicate FORSKA patches, which are collectively subject to a generalized stochastic process representing the disturbance regime.

The long time frame (centuries) and time step (ca. 1 year) of the model dictate that many of the processes involved are represented in a simpler way than would be appropriate for, say, a model whose primary aim was to simulate individual tree growth. Physiological processes are represented by simple equations whose most important characteristic is robustness over a wide range of species and environmental conditions, rather than precision over any particular range of species and conditions (cf. Running and Coughlan, 1988; Prentice and Helmisaari, 1991). The principle of model construction is quite general. However, the model in its present form is tailored to the simulation of forests in humid regions where competition for light is important while competition for water is unimportant. Modifications would be required if the model were to be applied to semi-arid forests. Waterlogged soils and permafrost dynamics, as modelled by Bonan (1989), are also not considered. Nutrient cycling is not explicitly modelled; we assume that changes in nutrient cycling are linked to changes in carbon cycling (Pastor and Post, 1988) and therefore to the basic successional dynamics, determined primarily by competition for light.

MODEL DESCRIPTION

Computation of environmental scalars

Growing degree-days (gdd)

Accumulated temperature during the growing season is an index of the energy available for completion of the annual life cycle (Woodward, 1987). Here, monthly temperature data for each year are interpolated linearly between mid-months to yield quasi-daily values T_i (°C) where i is the Julian date. The annual *gdd* (day °C) is

$$gdd = \Sigma_i \max\{0,(T_i - 5)\} \quad (1)$$

Soil moisture

Changes in the climatic water balance are transmitted to plants through soil, whose water holding capacity determines the extent to which moisture can be carried through into dry seasons. Soil moisture accounting is carried out in the simplest possible way, assuming a single water store from which runoff occurs only when the store is full. Monthly precipitation rate (mm day^{-1}) and sunshine (proportion of possible hours of bright sunshine) are interpolated in a similar way to temperature to yield quasi-daily values P_i (mm) and n_i, respectively. Daily soil moisture, Ω_i (mm), is updated by

$$\Omega_i = \min\{[\Omega_{i-1} + (P_i - E_i)], \Omega_{max}\} \quad (2)$$

where E_i is the actual daily evapotranspiration (AET) and Ω_{max} is the soil water capacity (difference between field capacity and wilting point). Snow is not differentiated. Soil moisture is set at Ω_{max} on day 1 of the first year of simulation. This is realistic for humid and northern winter- or southern summer-wet climates; elsewhere, Ω_1 normally converges to a value $< \Omega_{max}$ within 2–5 years.

AET is calculated by a method based on Federer (1982). We take the *instantaneous* AET, E, to be the lesser of a supply function S and a demand function D:

$$E = \min\{S, D\} \quad (3)$$

Following Federer (1982),

$$S = C_w(\Omega_{i-1}/\Omega_{max}) \quad (4)$$

i.e. the supply function is proportional to soil moisture, which does not change significantly during the day, and declines with relative soil wetness rather than absolute water content. C_w is the maximum evapotranspiration rate from saturated soils under conditions of high demand.

A demand function suitable for landscape-scale applications is motivated by the theory of equilibrium evapotranspiration (Jarvis and MacNaughton, 1986). According to this theory, small-scale spatial variations in evapotranspiration related to variations in stomatal and aerodynamic resistance cancel one another on spatial scales comparable with the scale of mixing in the planetary boundary layer (tens of km). When soil moisture is not limiting, the large-scale evapotranspiration rate is thus determined by the energy supply for evaporation. Atmospheric humidity adjusts on a time scale of minutes to hours so that the plant–atmosphere vapour pressure gradient, surface resistances and energy supply remain in balance. Following this theory, we equate instantaneous evaporative demand with the equilibrium evapotranspiration rate:

$$D = 3600[s/(s+\gamma)]R_n/L \quad (5)$$

(mm h^{-1}), where R_n is the instantaneous net radiation (W m^{-2}); s is the rate of increase of saturated vapour pressure with temperature, given by

$$s = 2.503 \times 10^6 \exp[17.269\ T_c/(237.3 + T_c)]/(237.3 + T_c)^2 \quad (6)$$

(Pa K^{-1}) where T_c is Celsius temperature; γ is the psychrometer constant, ca. 65 Pa K^{-1}; and L is the latent heat of vaporization of water, ca. 2.5×10^6 J kg^{-1}. Tables are used to take account of the weak dependence of γ and L on temperature.

The problem of estimating evaporative demand then becomes primarily the problem of estimating net radiation, R_n. Net radiation is the net downward short-wave flux R_s minus the net upward long-wave flux R_l. Following Linacre (1986), we take

$$R_s = (c + dn_i)(1 - \beta)Q_0 \cos z \quad (7)$$

where c and d are empirical constants ($c + d$ = the clear-sky transmittivity), β is the short-wave albedo,

$$Q_0 = Q_{00}[1 + 2 \times 0.01675 \cos(360i/365)] \quad (8)$$

where Q_{00} is the solar constant (1360 W m^{-2}), and

$$\cos z = \sin l \sin \delta + \cos l \cos \delta \cos h \quad (9)$$

where l is latitude,

$$\delta = -23.4° \cos[360(i + 10)/365] \quad (10)$$

and h is the time of day, in angular units from solar noon. The net upward long-wave flux can be approximated by a linear function of temperature over the limited range of absolute temperatures that occur near the earth's surface (Monteith, 1973). Again following Linacre (1986),

$$R_l = [b + (1 - b)n_i](A - T_c) \quad (11)$$

where b and A are empirical constants. T_c is equated with the mean daily Celsius temperature ($T_i - 273$) in eqns (6) and (11), i.e. we neglect the effects of diurnal temperature variations on s, γ, L and R_l. D is then a linear function of cos h. Integration of this function over the part of the day with $R_n > 0$ (with due attention to the special cases of polar day and night) yields the daily equilibrium evapotranspiration, D_i. E is integrated in a similar way to yield the daily AET, E_i. Nighttime condensation is assumed not to contribute significantly to the water balance.

Photosynthetically active radiation (PAR)

The instantaneous PAR flux density is taken as

$$I = (0.5/e^*)R_s \quad (12)$$

(μmol m^{-2} s^{-1}) where $e^* = 0.22$ MJ mol^{-1}. This makes the approximation that half the incoming short-wave radiation is PAR, and that there is no change in albedo or atmospheric absorption. Average daily PAR, I_i, is obtained by integrating the instantaneous PAR between sunrise and sunset and dividing by 86 400. The seasonal average PAR, $I(0)$, as used in the light competition calculations, is

$$I(0) = \Sigma_i I_i / g_s \tag{13}$$

where summation is over the period of g_s days with $T_i > 7.5$ (deciduous trees) or $T_i > 4$ (evergreens).

$I(0)$ depends on latitude and cloudiness. However, the dependence on latitude is weakened by the fact that the period g_s is shorter at high latitudes, and more concentrated in the months with long days and high insolation.

Environmental effects on forest processes

Effects of environment on assimilation, establishment and respiration rate are modelled by combining functions representing different environmental controls:

$$[m_G] = \delta_{tc-}\delta_{gdd-}\Phi_T\Phi_D\Phi_C \tag{14}$$

$$[m_E] = \delta_{tc+}\delta_{tw-}[m_G] \tag{15}$$

$$[m_R] = \mu_T \tag{16}$$

where the $[m_.]$ are composite multipliers; the δ are Kronecker delta functions taking the values 0 or 1, and the Φ and μ_T are non-negative, real-valued functions, as described below. Each of these functions can be "switched off" (set to unity) if required.

Thermal limits

Many species are restricted towards the poles and continental interiors by low-temperature damage (Woodward, 1987). Some species' range limits, e.g. the eastern limits of broad-leaved deciduous trees in Europe, can be correlated with isotherms of mean annual minimum temperature (Woodward, 1988) or mean temperature of the coldest month (Prentice and Helmisaari, 1991). Trees are also restricted poleward by growing-season heat requirements (Skre, 1972; Woodward, 1987) that can be correlated with *gdd*. Certain continental broad-leaved species are excluded from cool oceanic regions because their *regeneration* requires warm summers (Piggott and Huntley, 1981), and many conifers, especially, require cold winters for some aspect of regeneration.

For modelling purposes, these limits are represented by Kronecker delta functions affecting establishment and/or growth. The controlling variables are the temperature of the coldest month (*tc*), growing degree-days (*gdd*) and temperature of the warmest month (*tw*). Species are assigned a minimum *gdd* for growth. Below this limit, no growth can occur ($\delta = 0$); above this limit, growth is not limited by gdd ($\delta = 1$). Species are also assigned a minimum *tc* for growth. If no growth can occur, then no regeneration occurs either. Some species are assigned additional limits affecting regeneration only: a maximum value of *tc* and/or a minimum value of *tw*.

Effect of temperature on net assimilation

Within each species' range limits, growth is influenced by the effect of temperature on net assimilation and sapwood respiration. We compute a daily temperature response variable,

$$f(T)_i = 4(T_i - T_{\min})(T_{\max} - T_i)/(T_{\min} - T_{\max})^2 \tag{17}$$

which is a symmetrical parabola with a maximum value of 1 when $T_i = (T_{\min} + T_{\max})/2$. This is a reasonable approximation for the effect of temperature on net assimilation (Larcher, 1983). Annual net assimilation is reduced by a factor

$$\Phi_T = \Sigma_i f(T)_i/365 \tag{18}$$

where summation is over the period with $T_i > 5$ (deciduous trees) or $f(T)_i > 0$ (evergreens).

This formulation is simple, but more reasonable than the parabolic response of annual growth to *gdd* used in most gap models since Botkin et al. (1972). There is no evidence that annual growth should generally decline with increasing *gdd*. In particular, in situations where *gdd* increases due to an extension of the growing season, annual growth would generally be expected to increase, whereas a parabolic response to *gdd* could imply an unrealistic decrease.

Effect of temperature on sapwood respiration

Sapwood maintenance respiration is assumed to increase exponentially with temperature:

$$g(T)_i = Q_{10}^{(T_i - T_{\text{ref}})/10} \tag{19}$$

where T_{ref} is a reference temperature. We use $Q_{10} = 2.3$ and $T_{\text{ref}} = 5$. Annual sapwood respiration is then adjusted by a factor

$$\mu(T)_i = \Sigma_i g(T)_i/365 \tag{20}$$

Effect of drought

The soil moisture algorithm allows a variety of annual moisture indices to be calculated. We compute

$$\text{dri} = 1 - \Sigma_i E_i / \Sigma_i D_i \tag{21}$$

where summation is over the period with $T_i > 5$ (deciduous trees) or $f(T)_i > 0$ (evergreens). This index is the complement of the Priestley–Taylor coefficient (ratio of actual to equilibrium evapotranspiration), used here as an index of total drought stress, assessed over the assimilation period. Annual net assimilation is then reduced by a factor

$$\Phi_D = 1 - (\text{dri}/\text{dri}_{\max})^2 \tag{22}$$

i.e. a parabolic function (cf. Kercher and Axelrod, 1984) that takes the value 1 under no stress ($\text{dri} = 0$) and 0 at maximum tolerated stress ($\text{dri} = \text{dri}_{\max}$), with $\text{d}\Phi_D/\text{d}(\text{dri}) = 0$ at $\text{dri} = 0$ and becoming steeper towards $\text{dri}_{\max}$.

Direct CO_2 effects

Present understanding of direct effects of CO_2 changes does not allow reliable prediction at the level of whole tree or stand growth (Eamus and Jarvis, 1989). For completeness, our model nevertheless includes a caricature of a direct CO_2 effect consistent with the simplified, annual-average treatment of shading effects. Following Landsberg (1986), we start from a phenomenological model for net assimilation P,

$$P = P_{\max}(I - c)/(I + \alpha - c) \tag{23}$$

where I is the absorbed PAR and c is the PAR compensation point. $P_{\max}$ is the light-saturated net assimilation rate

$$P_{\max} = g_m(C_i - \Gamma) \tag{24}$$

where g_m is the mesophyll conductance, C_i is the internal CO_2 concentration, Γ is the CO_2 compensation point and α is a "half-saturation point" equal to $P_{\max}/\phi$, where ϕ is the quantum efficiency of photosynthesis. If we treat c, g_m, Γ and ϕ as constants and further assume a constant relationship

$$C_i = pC_a \tag{25}$$

where C_a is the ambient CO_2 concentration (e.g. Wong et al., 1979; Landsberg, 1986; Mohren, 1987), then a change in C_a would change both $P_{\max}$ and α by a factor

$$\Phi_C = 1 + p(C_a - C_{ao})/(pC_{ao} - \Gamma) \tag{26}$$

where C_{ao} is the present ambient CO_2. The model therefore applies the factor Φ_C both to annual net assimilation and to the half-saturation point, α.

With $\Gamma = 80$ ppm and $p = 0.7$, equation (26) gives a value of $\Phi_C = 2.53$ for a doubling of ambient CO_2 from 330 to 660 ppm. The effect on α however implies (a) that the growth increase would be considerably smaller (given that plants work at well below PAR saturation most of the time), and (b) that shade-tolerant plants (with low maximum net assimilation rates) would show a greater growth increase than shade-intolerant plants. This is consistent with Solomon's (1984) prediction that *low* CO_2 concentrations (e.g., at the last glacial maximum) favoured shade-intolerant trees. It is not known whether either prediction is true. However, experimental data cited by Bazzaz (1990, p. 185) suggest that seedlings of shade-tolerant tree species do show stronger growth enhancement than seedlings of shade-intolerant species, when grown in high CO_2.

The model does not include any direct effect of CO_2 on soil moisture. Equations (25) and (26) imply a decrease in stomatal conductance, to keep the assimilation rate consistent with the plant–atmosphere CO_2 gradient as ambient and internal CO_2 are raised. If ambient humidity remained unchanged, this decrease would imply less evapotranspiration, higher water-use efficiency and less effective drought. However, the theory of equilibrium evapotranspiration suggests that ambient humidity would decrease so as to leave evapotranspiration unchanged (Jarvis and MacNaughton, 1986). (Later critiques indicate that this may be an oversimplification, but it is accepted that such a feedback exists and that it substantially reduces the sensitivity of regional evapotranspiration to stomatal conductance.) Equation (5) allows us to apply climate change scenarios to the model without the need to assume an unchanged humidity, or to derive humidity (a mesoscale atmospheric variable that is highly dependent on land surface characteristics) from general circulation models that work at macroscale with highly simplified representations of the land surface.

Vegetation dynamics

Core model structure

Leemans and Prentice (1989) provided full documentation of FORSKA version 1. The "core" model used here differs only in a few details from that version. FORSKA simulates a mixed-species, mixed-age population of trees on a unit patch corresponding to the approximate area over which a tree influences its neighbours (ca. 0.1 ha). Each tree is described by its species, diameter at 1.3 m height (dbh), leaf area and bole height. Individual trees are not located spatially within the patch. The tree crowns are

treated as cylinders rather than as disks; competition for light is therefore typically less strongly asymmetric than in the models described by Shugart (1984).

The environmental routines are asynchronously coupled to the core model. Environmental information is calculated on a quasi-daily timestep and summarized in the form of annual scalars as described above. The core model updates the state description of the forest patches once every 1 or more years. With timesteps longer than 1 year, the annual environmental response scalars are averaged over the timestep length. We use a timestep of 2 years to allow trees to carry over resources from one year to the next, and so to be buffered to a certain extent against mortality due to a single climatically unfavourable year.

Light extinction

The trees shade themselves and each other according to the Lambert–Beer law:

$$I(z) = I(0)\ \mathrm{e}^{-kL_*(z)} \tag{27}$$

where $I(z)$ is the PAR at canopy depth z, k is an extinction coefficient and $L_*(z)$ is the accumulated leaf-area index (LAI) of all trees above depth z.

Allometry

Tree height, H, is derived from dbh, D, by a function with initial slope S_* and asymptote $H_{\max}$:

$$H = 1.3 + (H_{\max} - 1.3)\left\{1 - \exp\frac{-S_* D}{H_{\max} - 1.3}\right\} \tag{28}$$

The use of an asymptotic function, rather than the parabola used in most gap models, allows flexibility in the choice of functions used to describe growth.

Growth

Net growth is obtained by numerical integration through the crown of each tree. The function to be integrated expresses a balance between net assimilation by the leaves at each level, and the cost of maintaining a commensurate amount of sapwood up to that level; the higher the elevation of the leaves, the higher the sapwood cost, No maximum diameter is imposed, nor are trees constrained to stop growth when they reach maximum height.

The net assimilation rate at each level depends on the leaf-area profile and species-specific responses to shading, as well as other environmental effects expressed through the multiplier $[m_G]$. Net growth is further reduced as a decreasing function of total biomass, to account for nutrient depletion as the forest gains mass. The complete growth function is

$$\mathrm{d}(D^2H)/\mathrm{d}t = (1 - W/W_{\max}) \int_H^B s_L \{[m_G]\Gamma_* P(z) - [m_R] rz/C\} \, \mathrm{d}z \qquad (29)$$

where B is bole height, s_L is leaf area per unit height, W is biomass, $W_{\max}$ is a notional maximum biomass, Γ_* is proportional to the maximum net assimilation rate, r is proportional to the sapwood respiration rate, C is proportional to the ratio of leaf area to sapwood area, and

$$P(z) = [kI(z) - c]/[kI(z) + \alpha - c] \qquad (30)$$

where $kI(z)$ is the average PAR absorption by a given leaf layer, and c and α are the species' PAR compensation and half-saturation points, reflecting the species' shade tolerance. We use $\alpha = 330$ μmol m^{-2} s^{-1} for intolerants and 100 μmol m^{-2} s^{-1} for tolerants, with $c = 60$ μmol m^{-2} s^{-1} for intolerants and 10 μmol m^{-2} s^{-1} for tolerants. Biomass is the sum of stem dry weights w:

$$w = q\mathrm{D}^2H \qquad (31)$$

where q is a conversion constant incorporating both the wood density and form factor of the stems. Γ_* is most easily estimated from the annual diameter or height increment of young, unshaded trees growing under favourable environmental conditions (Moore, 1989; Prentice and Leemans, 1990). A value of r on the order of 0.02 year^{-1} gives reasonable stand carbon budgets for mesic forests in cool climates (Prentice and Leemans, 1990). Sensitivity analysis of FORSKA (Leemans, 1991a) showed that the precise values of r/C and $W_{\max}$ are unimportant, whereas Γ_*, C, c and α are important.

As in other gap models, the dbh increase during one timestep is derived by partitioning the volume index increment from equation (29) into height and diameter growth using the derivative of the relationship between height and dbh (Botkin et al., 1972). The model performs these manipulations explicitly in order to allow changes in the growth or height–diameter formulations to be made in a consistent manner.

Leaf-area dynamics

Leaf area is always assumed to be proportional to sapwood area, and newly established trees have leaf area

$$L = CD^2 \qquad (32)$$

where C is a species-specific constant that can be derived from measurements of the leaf-area/sapwood-area ratio or from measurements of leaf area and dbh in young trees. Sapwood area is assumed to convert to heartwood at a rate t_{sw} (ca. 0.04 year^{-1}). The rate of change of leaf area is therefore given by

$$dL/dt = 2CD(dD/dt) - t_{sw}L \tag{33}$$

which is used to update the leaf area in each timestep. Leaf area is assumed to be uniformly distributed within the crown, hence $s_L = L/(H - B)$.

Newly established trees have zero bole height; leaf area can later be reduced by self-pruning. After the new leaf-area profile is calculated, bole heights are raised (irreversibly), as necessary, to ensure that $P(z) > 0$ for all leaves. This mechanism generates qualitatively reasonable vertical leaf-area profiles after canopy closure in stands of mixed shade-tolerant and shade-intolerant trees (Leemans and Prentice, 1987; Prentice and Leemans, 1990).

Establishment

For each species, on each patch and at each timestep, the number of new saplings to be added to the tree population is drawn from a Poisson distribution with expectation $(\delta t.\text{est}/A_p)[m_E]P_f$ where est is the rate of establishment under optimal conditions (in ha^{-1} year^{-1}), δt is the timestep length, A_p is the area of the patch and P_f is the value of equation (30) at the forest floor. This formulation takes some account of the factors tending to reduce sapling establishment rate under conditions unfavourable for growth, including deep shade. The dbh of each new sapling is 1 cm, plus a uniformly distributed random fraction of the full dbh increase that the sapling could achieve in one timestep under the current environmental conditions at the forest floor.

Mortality

Mortality rates are inversely related to growth efficiency (stem volume increment per unit leaf area: Waring, 1983), rather than to dbh increment as in conventional gap models. The relative growth efficiency (E_{rel}) of a tree is the ratio of realized growth efficiency, E_{rea}, to the maximum for the species:

$$E_{max} = \Gamma_* P(0) \tag{34}$$

where $P(0)$ is the value of equation (30) for $z = 0$. Mortality occurs at a low rate X_{min} (inversely related to the species' maximum longevity) in vigorous trees, and at a much higher rate $(X_{min} + X_{max})$ in suppressed trees, i.e.

trees with $E_{rea} < E_{thr}$ where E_{thr} is a prescribed threshold value. Suppression can be a result of competition from other trees, or of an unfavourable environment. Each tree has probability of mortality $(1 - e^{-X \cdot \delta t})$ during each timestep, where X is the currently computed mortality rate applying to that tree.

Sprouting

Any tree that has been killed is checked to see if it is (a) of a species that can sprout, and (b) larger than the minimum size for sprouting. If so, the dead tree is replaced by a number of sprouts drawn from a Poisson distribution with expectation $\delta t.\text{spr}.E_{rel}$ where spr is a maximum sprouting rate (year^{-1}). This formulation ensures that trees that are killed as a result of shading, or unfavourable environment, are less likely to sprout than trees that were vigorous when they died.

Disturbance regime

Disturbance regimes in forest landscapes may be natural (e.g., windstorms and fires) or artificial (e.g., logging). Both share a general tendency for the probability of disturbance on a given patch of forest to increase with the successional age of the patch (Clark, 1989, 1990). Disturbance rates, whether natural or artificial, are often such that "old-growth" forests typically occupy only a small fraction of the landscape.

We implemented a generic disturbance regime as a family of stochastic processes with a hazard function (conditional probability of disturbance) given by

$$Y = \sigma t^{\sigma-1}/t_*{}^{\sigma} \tag{35}$$

where t_* is a time constant and t is the successional age of the patch. This specifies a Weibull probability distribution of disturbance (Clark, 1989). If $\sigma = 1$, the hazard is independent of age. The probability of disturbance during a finite timestep of length δt is then $1 - \exp(-\delta t/t_*)$, and t_* is then simply the average interval between disturbances. With $\sigma = 2$ as used here, the hazard increases linearly with age; the probability of disturbance during a discrete timestep becomes $1 - \exp[(t_0/t_*)^2 - (t_1/t_*)^2]$, where t_0 is the beginning and t_1 is the end of the timestep. t_* is now the root-mean-square interval between disturbances. Disturbance is modelled as the removal of all trees from the patch.

RESULTS AND DISCUSSION

The behaviour of the model is illustrated with a simulation of typical forest landscapes in central Sweden, within the boreonemoral ecotone

TABLE 1

Model and site parameters

Site parameters		
Ω_{max}	Soil water capacity (good soil)	180 mm
	(poor soil)	90 mm
C_w	Maximum AET	1.0 mm h^{-1}
β	Albedo	0.17
W_{max}	Maximum biomass	600 Mg ha^{-1}
Model parameters		
c		0.25
d		0.5
b		0.2
A		107 W m^{-2}
	Number of patches	200
A_p	Patch size	0.1 ha
δt	Time step	2 years
	Vertical integration step	0.5 m
k	Light extinction coefficient	0.4
T_{ref}	Reference temperature	5°C
t_*	Disturbance return time	100 years
σ		2
X_{max}	Mortality rate of suppressed trees	0.46 $year^{-1}$

region (in North American terms, the transition between boreal and northern hardwood forests), which is likely to be especially strongly affected by global warming (Solomon, 1986; Pastor and Post, 1988; Prentice et al., 1991c). Model and site parameters are listed in Table 1. Silvics data from Prentice and Helmisaari (1991) were used to generate the species parameter values, by methods described in Prentice and Leemans (1990). The model was initially run with climate data for Stockholm (59°21'N; Table 2) on soils with water capacity values typical of "good" (loam) and "poor" (sandy) soils in the region. The model was initialized with bare

TABLE 2

Climate data for Stockholm

	J	F	M	A	M	J	J	A	S	O	N	D
T [a]	−2.9	−3.1	−0.7	4.4	10.1	14.9	17.8	16.6	12.2	7.1	2.8	0.1
P [b]	43	30	26	31	34	45	61	76	60	48	53	48
n [c]	20	31	42	49	57	59	54	52	46	33	18	14

[a] Mean daily temperature (°C).

[b] Mean precipitation (mm).

[c] Mean sunshine (% of daylight hours).

TABLE 3

Climate changes for central Sweden, based on a GISS GCM simulation of the effects of a CO_2 doubling

	DJF	MAM	JJA	SON
Temperature change (°C)	5.1	4.0	2.2	3.8
Precipitation change (mm day^{-1})	0.4	0.6	0.7	0.5

ground and run for 400 years to allow it to reach equilibrium in a constant climate.

The composition of forests in the Stockholm district, as recorded by the Swedish national forest inventory service, is within the range of the equilibrium compositions simulated for these two soil types by this method (Prentice et al., 1991c). The same procedure also generated reasonably good estimates of composition and biomass for forests in a range of cool climates, from northern boreal forest in northern Sweden (Prentice et al., 1991c) to temperate deciduous forest in southern Sweden (Prentice et al., 1991c) and northern France (Sykes, unpublished results).

A scenario of climate change for central Sweden was derived from results obtained with the GISS general circulation model for a doubling of atmospheric CO_2 (Hansen et al., 1984; Boer et al., 1990). Table 3 shows anomalies (differences between the simulated $2 \times CO_2$ climate and the simulated present climate) for each season. These anomalies were added to the corresponding monthly temperature and/or precipitation data to obtain a "greenhouse" climate whose closest present European analog is in northern France. Direct CO_2 effects were switched off throughout the simulation; thus the results indicate what might happen simply as a result of CO_2-induced climate change, with no consideration of the direct physiological effects of increasing CO_2. The changes were started at year 400 and allowed to take place linearly over 100 years; the model was then allowed to relax towards a new equilibrium in the warmer climate.

Figure 1 shows the time course of simulated biomass of the main tree species in these experiments, starting 100 years before the start of the climate change and continuing for 200 years after the climate change was complete. For two of these experiments, temperature and precipitation were changed according to Table 3. For the other two, temperature alone was changed.

The contrast between the first 100 years of simulation shown in Fig. 1 for good and poor soils reflects a contrast that is obvious on the present-day landscapes of central Sweden. Deeper and more silt- and clay-rich soils support *Picea abies* (Norway spruce) as the dominant in all but early-

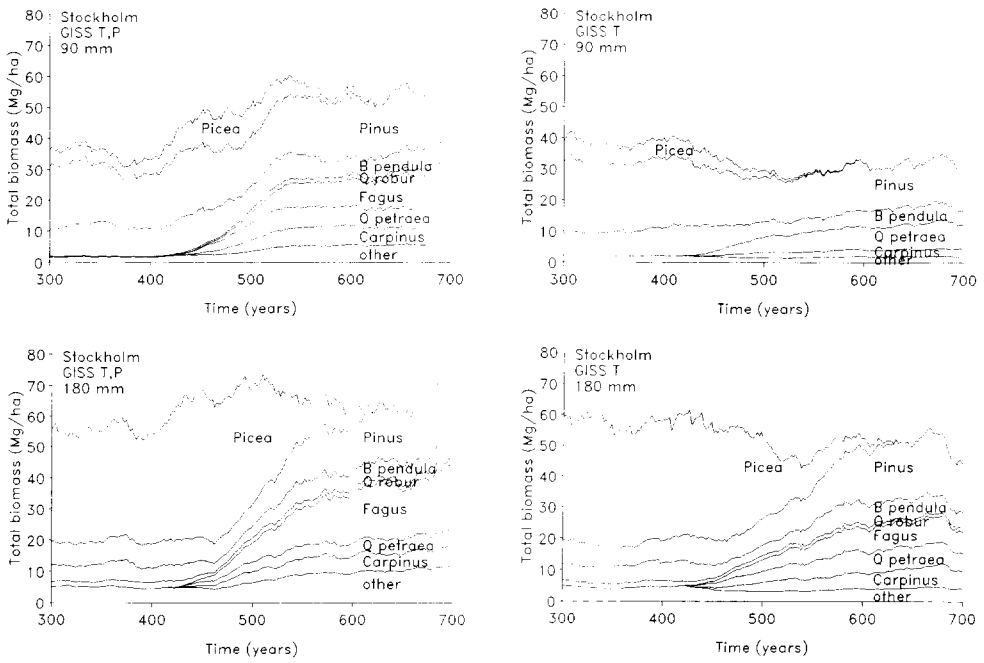

Fig. 1. Simulated changes in forest composition for soils of different water-holding capacity in the Stockholm region. T = temperature alone changed; T,P = temperature and precipitation changed. Climate changes (Table 3) took place by linear increments between years 400 and 500 of each simulation; thereafter, climate remained constant at the new level.

successional patches (Prentice and Leemans, 1990), while on the shallower and sandier soils standing biomass is less and *Pinus sylvestris* (Scots pine) dominates regardless of successional age.

In all four experiments, the climate changes produce the effect noted by Prentice et al. (1991c): gradual elimination of *Picea* due to a failure of regeneration in the warm winters of the "greenhouse" climate. All four runs also show the appearance and gradual increase in abundance of *Carpinus betulus* (hornbeam) and *Quercus petraea* (sessile oak), species whose growing-season warmth requirements are not satisfied in the Stockholm region today. On the good soils, and on poor soils when precipitation is increased along with temperature, these newcomers are joined by *Fagus sylvatica* (beech).

The effect of the precipitation increases is slight on the good soils; the most obvious effects are the slight decline in average forest biomass if temperature alone is raised (the combination of temperature and precipitation increases allows a slight increase in biomass), and a difference in the abundance of *Fagus* between the two scenarios. On the poor soils, how-

ever, the difference is substantial; without the precipitation increase *Picea* is eliminated more rapidly than in the other experiments, *Fagus* does not appear, and biomass declines sharply in contrast with the large increase permitted when temperature and precipitation increase together. These results confirm an intuitive expectation that in an area where drought can today be a limiting factor for forest production and a determinant of local species composition, the effects of rising temperature include declines in biomass and production (with concomitant effects on species composition) unless the temperature changes are offset by increases in precipitation. These effects are shown to be more drastic on the poorer soils, which store less water and therefore run a greater risk of drought.

We also ran a parallel set of simulations in which the direct effects of CO_2 on growth, as caricatured in the model, were allowed to take effect as CO_2 rose linearly from 330 ppm during the first 400 years to 660 ppm at 500 years (results not shown). The simulated compositional changes, and the rate at which they occurred, were similar to those produced by climate change alone. The differences were (a) in total biomass and production, which generally rose with increasing CO_2, and (b) in the quantitative balance of species, with shade-tolerant species (especially *Picea* and *Fagus*) accounting for a disproportionate share of the CO_2-induced increase in biomass.

The model in its present form does not allow investigation of the effects of possible increases in water-use efficiency, but any such increases would presumably have reduced the sensitivity of the simulated changes to soil water capacity, increased biomass on poor soils, and lessened the amount of precipitation required to offset temperature-induced summer drought. Such direct CO_2 effects are secondary in comparison with the changes predicted to occur as a result of CO_2-induced changes in climate in this region.

This application illustrates the model's ability to simulate the landscape-average equilibrium composition of forests and their transient behaviour in a particular region and under a specified climatic scenario. The model may also be used in similar fashion to explore the sensitivity of forests of different regions to climate changes of different directions, magnitudes and rates. The model's structure is sufficiently explicit and modular to allow direct CO_2 effects, and their interactions with climatic effects, to be modelled more realistically as understanding of these processes develops.

ACKNOWLEDGMENTS

This research was supported by grants from the Swedish Natural Science Research Council (NFR) to the project "Simulation modelling of natural

forest dynamics". We thank especially Pat Bartlein, Bhaskar Choudhury, Sandy Harrison, Henry Nix, Hank Shugart, Al Solomon and Ian Woodward for advice and encouragement.

REFERENCES

Bazzaz, F.A., 1990. The response of natural ecosystems to the rising global CO_2 levels. Annu. Rev. Ecol. Syst., 21: 167–196.

Boer, M.M., Koster, E.A. and Lundberg, H., 1990. Greenhouse impact in Fennoscandia—preliminary findings of a European workshop on the effects of climatic change. Ambio, 19: 2–10.

Bolin, B., Döös, B.R., Jäger, J. and Warrick, R.A., 1986. The Greenhouse Effect, Climatic Change, and Ecosystems. Wiley, Chichester, 541 pp.

Bonan, G.B., 1989. A computer model of the solar radiation, soil moisture, and soil thermal regimes in boreal forests. Ecol. Modelling, 45: 275–306.

Bonan, G.B. and Shugart, H.H., 1989. Environmental factors and ecological processes in boreal forests. Annu. Rev. Ecol. Syst., 20: 1–28.

Botkin, D.B., Janak, J.F. and Wallis, J.R., 1972. Some consequences of a computer model of forest growth. J. Ecol., 60: 849–873.

Clark, J.S., 1989. Ecological disturbance as a renewal process: theory and application to fire history. Oikos, 56: 17–30.

Clark, J.S., 1990. Fire and climate change during the last 750 yr in northwestern Minnesota. Ecol. Monogr., 60: 135–159.

Desanker, P.V. and Prentice, I.C., 1991. A vegetation dynamics model for the miombo woodlands of Zambezian Africa. Unpublished manuscript.

Eamus, D. and Jarvis, P.G., 1989. The direct effects of increase in the global atmospheric CO_2 concentration on natural and commercial trees and forests. Adv. Ecol. Res., 19: 2–55.

Federer, C.A., 1982. Transpirational supply and demand: plant, soil, and atmospheric effects evaluated by simulation. Water Resour. Res., 18: 355–362.

Hansen, J., Lacis, A., Rind, D., Russell, G., Stone, P., Fung, I., Ruedy, R. and Lerner, J., 1984. Climate sensitivity: analysis of feedback mechanisms. In: J.E. Hansen and T. Takahashi (Editors), Climate Processes and Climate Sensitivity. Geophys. Monogr., 29: 130–163.

Houghton, J.T., Jenkins, G.J. and Ephraums, J.J., 1990. Climate Change: The IPCC Scientific Assessment. Cambridge University Press, Cambridge.

Huntley, B. and Webb, T., III, 1988. Vegetation History. Kluwer, Dordrecht, 803 pp.

Jarvis, P.G. and McNaughton, K.G., 1986. Stomatal control of transpiration: scaling up from leaf to region. Adv. Ecol. Res., 15: 1–49.

Kercher, J.R. and Axelrod, M.C., 1984. A process model of fire ecology and succession in a mixed-conifer forest. Ecology, 65: 1725–1742.

Landsberg, J.J., 1986. Physiological Ecology of Forest Production. Academic Press, New York.

Larcher, W., 1983. Physiological Plant Ecology, 2nd edn. Springer-Verlag, Berlin, 303 pp.

Leemans, R., 1991a. Sensitivity analysis of a general forest succession model. Ecol. Modelling, 53: 247–262.

Leemans, R., 1991b. Simulation and future projection of succession in a Swedish broad-leaved forest. For. Ecol. Manage., 48: 305–319.

Leemans, R. and Prentice, I.C., 1987. Description and simulation of tree-layer composition and size distributions in a primaeval *Picea–Pinus* forest. Vegetatio, 69: 147–156.

Leemans, R. and Prentice, I.C., 1989. FORSKA, a general forest succession model. Meddelanden från Växtbiologiska institutionen, Uppsala (ISSN 0348-1417), 1989 (2).

Linacre, E.T., 1986. Estimating the net-radiation flux. Agric. Meteorol., 5: 49–63.

Mohren, G.M.J., 1987. Simulation of Forest Growth. Ph.D. Thesis, Agricultural University, Wageningen, 184 pp.

Monteith, J.L., 1973. Principles of Environmental Physics. Arnold, London.

Moore, A.D., 1989. On the maximum growth equation used in forest gap simulation models. Ecol. Modelling 63–67.

Pastor, J. and Post, W.M., 1988. Response of northern forests to CO_2-induced climate change. Nature, 334: 55–58.

Pickett, S.T.A., 1980. Non-equilibrium coexistence of plants. Bull. Torrey Bot. Club, 107: 238–248.

Pickett, S.T.A. and Thompson, J.N., 1978. Patch dynamics and the design of nature reserves. Biol. Conserv., 13: 27–37.

Pickett, S.T.A. and White, P.S., 1985. The Ecology of Natural Disturbance and Patch Dynamics. Academic Press, New York.

Piggott, C.D. and Huntley, J.P., 1981. Factors controlling the distribution of *Tilia cordata* at the northern limits of its geographical range. I. Distribution in north-west England. New Phytol., 84: 145–164.

Prentice, I.C., 1991. Climate change and long-term vegetation dynamics. In: D.C. Glenn-Lewin, R.K. Peet and T.T. Veblen (Editors), Vegetation Dynamics Theory. Chapman and Hall, in press.

Prentice, I.C. and Helmisaari, H., 1991. Silvics of north European trees: compilation, comparisons and implications for forest succession modelling. For. Ecol. Manage., 42: 79–93.

Prentice, I.C. and Leemans, R., 1990. Pattern and process and the dynamics of forest structure: a simulation approach. J. Ecol., 78: 340–355.

Prentice, I.C., Monserud, R.A., Smith, T.M. and Emanuel, W.R. 1991a. Modelling global vegetation change. In: A.M. Solomon and H.H. Shugart (Editors) Vegetation Dynamics and Global Change. Cambridge University Press, Cambridge, in press.

Prentice, I.C., Bartlein, P.J. and Webb, T., III, 1991b. Vegetation and climate changes in eastern North America since the last glacial maximum. Ecology, 72: 2038–2056.

Prentice, I.C., Sykes, M.T. and Cramer, W., 1991c. The possible dynamic responses of northern forests to global warming. Global Ecol. Biogeogr. Lett., 1: 129–135.

Running, S.W. and Coughlan, J.C., 1988. A general model of forest processes for regional applications. I. Hydrologic balance, canopy gas exchange and primary production processes. Ecol. Modelling, 42: 125–154.

Shugart, H.H., 1984. A Theory of Forest Dynamics. Springer-Verlag, New York.

Skre, O., 1972. High temperature demands for growth and development in Norway spruce (*Picea abies* (L.) Karst.) in Scandinavia. Meld. Nor. Landbrukshögsk., 51(7): 1–29.

Solomon, A.M., 1984. Forest responses to complex interacting full-glacial environmental conditions. AMQUA Abstracts, 8: 120.

Solomon, A.M., 1986. Transient responses of forests to CO_2-induced climatic change: simulation modelling experiments in eastern North America. Oecologia, 68: 567–579.

Waring, R.H., 1983. Estimating forest growth and efficiency in relation to canopy leaf area. Adv. Ecol. Res., 13: 327–354.

Webb, T., III, 1986. Is vegetation in equilibrium with climate? How to interpret late-Quaternary pollen data. Vegetatio, 67: 75–92.

White, P.S., 1979. Pattern, process and natural disturbance in vegetation. Bot. Rev., 45: 229–299.

Woodward, F.I., 1987. Climate and Plant Distribution. Cambridge University Press, Cambridge.

Woodward, F.I., 1988. Temperature and the distribution of plant species. In: S.P. Long and F.I. Woodward (Editors), Plants and Temperature. Symp. Soc. Exp. Biol., 42: 59–75.

Wong, S.C., Cowan, I.R. and Farquhar, G.D., 1979. Stomatal conductance correlates with photosynthetic capacity. Nature, 282: 424–426.